

Influence of pH on the Composition, Morphology and Corrosion Resistance of Zn-Ni-Mn Alloy Films Synthesized by Electrodeposition

Mortaga M. Abou-Krishna^{1,2,*}, Mohamed I. Attia², Fawzi H. Assaf¹ and Ahmed A. Eissa¹

¹ Faculty of Science, Chemistry Department, South Valley University, Qena, 83523, Egypt.

² College of Science, Chemistry Department, Al Imam Mohammad Ibn Saud Islamic University (IMSIU), Riyadh 11623, KSA.

*E-mail: m_abou_krishna@yahoo.com

Received: 31 December 2014 / Accepted: 23 January 2015 / Published: 24 February 2015

In this work, the effect of electrolyte pH on the composition and microstructure of Zn-Ni-Mn films were investigated using EDS, XRD and SEM. The composition of Zn-Ni-Mn films are greatly affected by the electrolyte pH. Low electrolyte pH (≤ 1) favors the normal deposition with very low amounts, while higher electrolyte pH leads to the anomalous deposition which decreases with increasing pH. The films prepared at low pH values show a very poor quality with rough surface while those electrodeposited at high pH value (2.5~5) are generally quite smooth, uniform and compact. Galvanostatic measurements for electrodeposition, cyclic voltammetry (CV) were used to the anodic and cathodic behavior of alloy to study the potential ranges. Anodic linear sweep voltammetry (ALSV) technique was used for the phase structure determination. The effect of pH on the film quality and corrosion performances in the films, the corrosion test was performed by the potentiodynamic anodic polarization method. The corrosion resistance of the coating films was increased towards pH = 2.5 and then decreased with increasing pH value of the electrolyte.

Keywords: Zn-Ni-Mn film; Corrosion resistance; Electrochemical deposition; Electrolyte pH; Anomalous codeposition

1. INTRODUCTION

Corrosion is generally defined as the gradual destruction of materials (usually metals) by chemical reaction with their environment. The coatings can protect the metal substrates, from corrosion, by two main mechanisms: sacrificial and barrier protection mechanisms. Conventional Zn coatings for corrosion resistance is not enough due to the permanent need of industry to diminish the

coating thickness and to increase corrosion resistance at the same time. Zn coatings were replaced by Zn alloys in development of highly corrosion resistant coatings on. [1-5]

Electrodeposition of Zn with Fe-group metals are classified as anomalous codeposition, since the less noble Zn deposits preferentially in most plating conditions. Different hypotheses found in the literature to explain this anomaly. [6-9]. In electrodeposition the growth mechanism, morphology and micro-structural properties of the film depend on electrodeposition conditions such as electrolyte pH.

Electrodeposited Zn-Ni alloys have greater corrosion protection, improved mechanical properties and better thermal stability as compared to bare zinc and other zinc alloy coatings [10]. Zn-Mn alloy electrodeposition are of growing interest because of their superior protective properties [11,12]. Low manganese content coatings have shown better mechanical properties needed for automotive applications as well as steel protection in different aggressive environments. It is expected that, it will be important to accumulate the properties of Zn-Ni and Zn-Mn binary alloys in one alloy through the electrodeposition of Zn-Ni-Mn ternary alloy.

The pH affects greatly the electrodeposition of alloys [13-16]. In the present work, the composition, morphology and corrosion resistance of electrodeposited Zn-Ni-Mn films will be investigated as a function of the pH values in electrolyte.

2. EXPERIMENTAL

The chemical composition of the basic electrolyte of Zn-Ni-Mn bath is ZnSO₄ [0.10 M], NiSO₄ [0.10 M], MnSO₄ [0.10 M], Na₂SO₄ [0.20 M], H₃BO₃ [0.20 M] and different concentrations of H₂SO₄. The electrolytes and all used solutions were freshly prepared using double distilled water from Analar grade. All experiments were carried out in duplicated and the reproducibility of these measurements was found satisfactory. For a standard bath deposition, a series of experiments at different times were carried out and the relative standard deviation (RSD%) was found to be 3.5, 2.7 and 4.4% for the Zn, Ni and Mn contents in the deposit, respectively.

Electrochemical measurements were performed using EG&G Potentiostat/Galvanostat model 273A controlled by a PC using 352 corrosion software. The electrochemical corrosion measurements of the coatings; polarization resistance (R_p), corrosion potential ($E_{corr.}$) corrosion current density (i_{corr}) achieved and denoted in Table (1).

In the cyclic voltammetric technique, the potential applied to the working electrode is scanned linearly from an initial value 0.0 mV to a second value -1300 mV then back to 0.0 mV. The galvanostatic measurements were conducted by keeping the current density of cathodes in the examined solution at a constant level, 10 mA cm⁻², for 10 minutes. In the potentiostatic measurements were directed by possession the potential of cathodes in the studied solution at -1300 mV in 10 minutes. The electrodeposition process was usually performed at H₂SO₄ concentration = 0.01 M, while investigating the influence of pH, the electroplating was carried out at different H₂SO₄ concentrations.

The chemical composition of Zn-Ni-Mn deposits were determined using atomic absorption spectroscopy (Thermo scientific, model ICE 3000 series AA spectrometer). These data were used to calculate the efficiency of the process. The deposited layer of Zn-Ni-Mn alloy was dissolved in 50.0

cm³ of 20% HCl solution, and the suitable diluted solution was then analyzed to find out the Zn, Ni and Mn contents in the deposited alloy. The cathode current efficiencies of pure Zn, Ni and Mn were determined according to Faraday's laws as detailed in Ref. [17]

The X-ray diffraction patterns of the obtained deposits were recorded with a Bruker AxS-D8 Advance X-ray diffractometer using Cu-K α radiation, to find the different deposited alloy phases. The surface morphology of the deposit is evaluated by using a scanning electron microscope, (JSM-5500 LV, SEM, JEOL, Japan). The Zn and Ni content in the deposit have been confirmed by EDS (Energy Dispersive X-ray Spectrometer) system with link Isis software and model 6587 An X-ray detector (OXFORD, UK). The thickness of the deposited alloy layer has been approximately estimated from the amount of deposit and the densities of Zn ($d_{Zn}=7.14 \text{ g cm}^{-3}$), Ni ($d_{Ni}=8.90 \text{ g cm}^{-3}$) and Mn ($d_{Mn}=7.21 \text{ g cm}^{-3}$) [17,18] and confirmed by SEM (cross-section). The experiments have been done without cathode movement or solution agitation.

3. RESULTS AND DISCUSSION

3.1 Cyclic Voltammetry

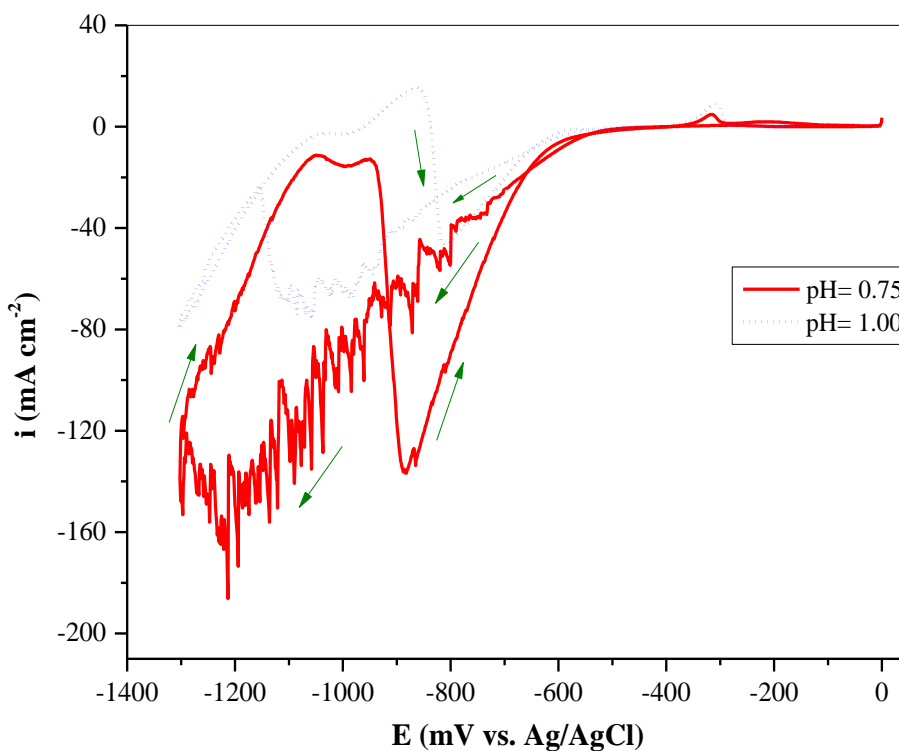


Figure 1.a. CV curves for steel at 5 mV/s and 25.0 °C in a standard bath at pH values of 0.75 and 1.

The pH value of the electrolyte from which the coatings are obtained is one of the most important variables during the electrodeposition process since it largely affects the composition,

appearance and corrosion resistance properties of these coatings. Figure (1.a) exhibits the cyclic voltammograms for Zn-Ni-Mn alloys on steel rod at pH values of 0.75 and 1. In the cathodic part of the cyclic voltammogram at pH of 0.75, the cathodic peak, which starts at about -543 mV is ascribed to the co-deposition of sulfur liberated from the reduction of sulfate group of sulfuric acid at the cathode surface [19]. Fortunately, the co-deposition of sulfur may lead to the improvement of the deposits crystallinity [20]. As the potential shifts to more negative values, the current density shifts rapidly to more cathodic values with great fluctuations due to the deposition of alloy components combined with the intense hydrogen evolution reaction which seems to be responsible for these great fluctuations since the acidity of the electrolyte is high (pH is low).

Switching of the direction of the potential scan (CV at pH=0.75) to the positive direction at -1300 mV, there are two abnormal peaks at -1045 and -953 mV and normal peak is found at -316 mV. It is apparent that, the current density in the first two peaks is still remaining negative, because the cathodic reduction of H^+ and H_2O are still ongoing. The dissolution of a small amount of the alloy does not bring the current density back to positive. The deposition of small amounts of the deposit is related to the high acidity of the electrolyte from which the deposit is obtained, leading to dissolution to a part of the deposit during its deposition. The third anodic peak in which the current density becomes positive is attributed to the dissolution of previously deposited nickel from its phases. It is surprising to observe that the second peak is accompanied by a reduction peak during the anodic scan. In other studies, a reduction peak during the oxidation of Zn-Ni alloys has been observed and has been attributed to the hydrogen evolution due to the low pH value used (pH= 1.6) [21,22]. However, in another study for Zn-Ni alloys performed in a weakly acidic electrolyte (pH= 5.6), the reduction process observed during the oxidation of these alloys has been ascribed to the deposition of nickel, together with some hydrogen evolution, [10] in accordance with the present study at lower pH values, where the results of the deposit analysis before and after the reduction peak demonstrates that, this observed reduction process during the positive scan is related to the deposition of nickel combined with some hydrogen evolution.

The cyclic voltammogram at pH of 1.0 is similar to that obtained at pH of 0.75 except in the following: firstly, the deposition of sulfur together with hydrogen evolution starts at a more negative value which is -561 mV, secondly, the fluctuations observed in the cathodic part of the voltammogram are less than those obtained at pH of 0.75 due to the lower pH value in this case. This confirms that, these fluctuations are correlated to the hydrogen evolution reaction. The third exception is the height of the anodic peaks increasing and the peaks shift towards the positive direction where they become at -1031, -863 and -310 mV, fourthly, the current density of the first dissolution peak remains negative meanwhile that of the second one becomes positive, indicating the higher amount of alloy components deposited in this case which are sufficient to make the current density positive during the anodic scan. Last exception is the intensity of the reduction peak observed during the anodic scan decreases, and that is due to the lower pH value which confirms that the magnitude of this peak is correlated to the hydrogen evolution reaction. Moreover, it shifts towards the positive direction, and that may be ascribed to the deposition of the single metals from the deposit.

Figure (1.b) shows the cyclic voltammograms for Zn-Ni-Mn alloys on steel rod at different pH values ranging from 1.5 to 5. At pH of 1.5, the deposition of sulfur together with hydrogen evolution begins nearly at -548 mV.

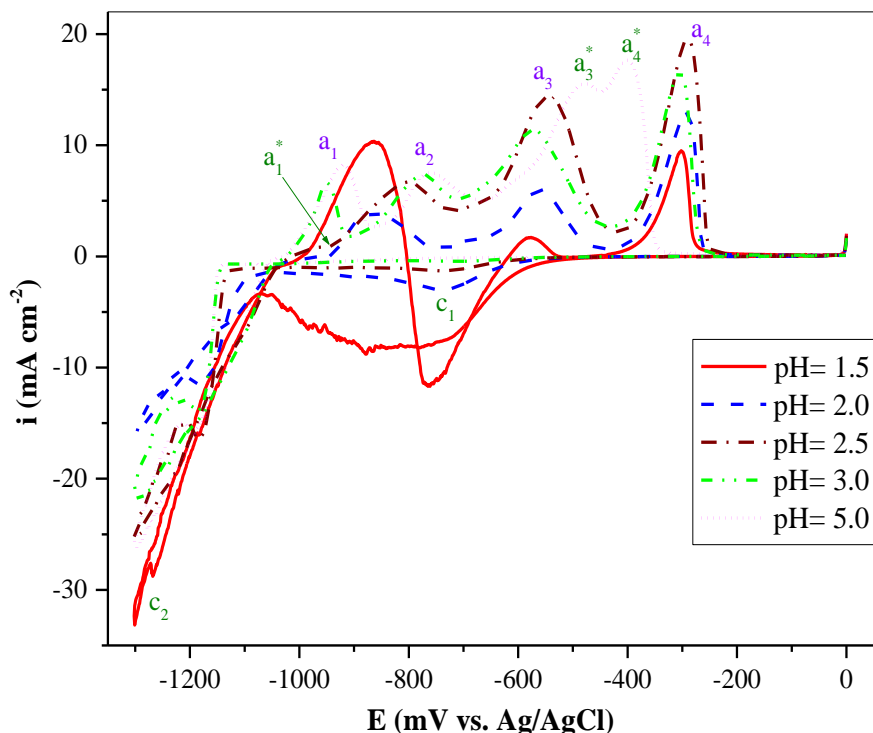


Figure 1.b. CV curves for steel at 5 mV/s and 25.0 °C in a standard bath at different pH values ranging from 1.5 to 5.

The plateau during the negative scan in the potential range from -702 to -1077 mV may be attributed to the continuously hydrogen evolution reaction. At potential of the -1077 mV, there is a sharp increment in the cathodic current density referring to the deposition of alloy components of this potential value resulting in the cathodic peak (c_2). During the anodic scan, there is a small shoulder at -1040 mV and three dissolution peaks at -867, -579 and -302 mV. The shoulder in which the current density remains negative is ascribed to the dissolution of manganese from its phases. This is due to the dissolution of a small amount of the manganese deposited here is not sufficient to bring the current density back to positive. The three anodic peaks relate to the dissolution of Zn from pure zinc phase, the dissolution of Zn from γ -Ni₅Zn₂₁ and/or δ -Ni₃Zn₂₂ phases (Figure 2) and the dissolution of Ni from nickel phases. It is clear that the reduction process during the positive scan is still occurring here.

At pH of 2 and 2.5, the deposition of sulfur is indicated by the cathodic peak (c_1) while the deposition of the alloy components begins at -1079 and -1127 mV respectively. It is clear that the intensity of the cathodic peak (c_1) decreases as the pH is increased from 2 to 2.5 due to the decrease in sulfuric acid concentration. On the anodic-going to scan, there is an anodic current shoulder (a_1^*) and

three anodic current peaks (a_2 , a_3 , and a_4) which correspond to the dissolution of the deposited alloy metals from their different phases.

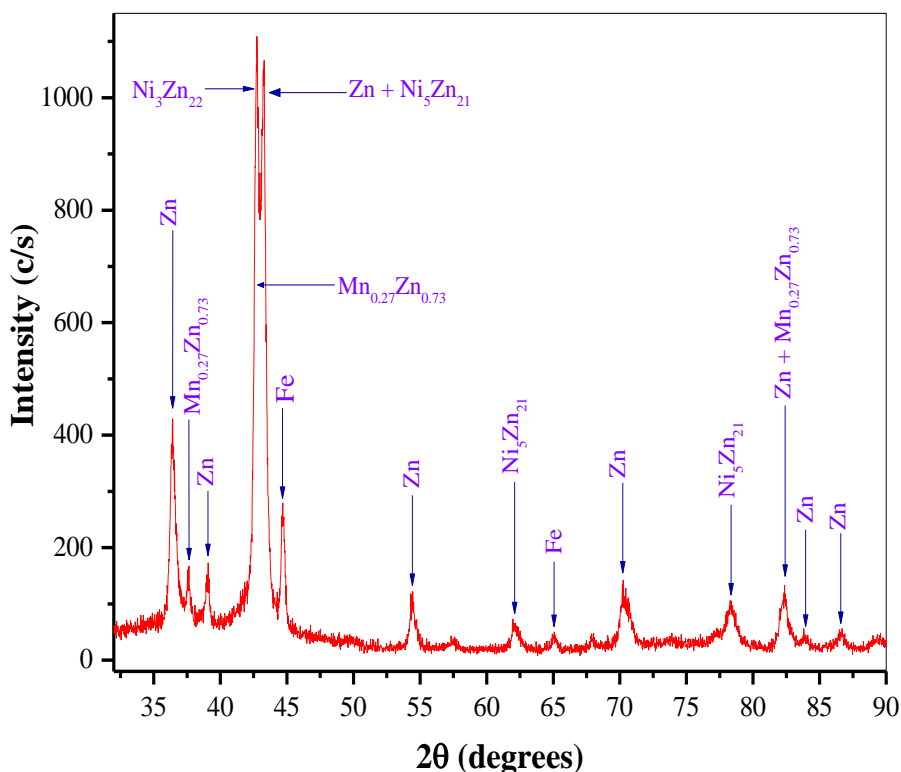


Figure 2. XRD peaks for Zn-Ni-Mn alloy electrodeposited on steel substrate of area 2 cm^2 at 10 mA cm^{-2} and $25.0 \text{ }^\circ\text{C}$ for 10 minutes from a standard bath.

At a pH of 3 and 5, the cathodic peak (c_1) has disappeared due to the low concentration of sulfuric acid confirming that this peak is correlated to the deposition of sulfur liberated from the reduction of sulfate group in the presence of sulfuric acid surface. [19]

It is noticeable that the deposition of the alloy components begins at nearly the same potential which is -1140 mV , which refers to that the alloys electrodeposited at pH values of 3 and 5 may have the same composition. On the anodic-going to scan at pH of 3, it is clear that there are four dissolution current peaks (a_1 , a_2 , a_3 , and a_4) at -950 , -774 , -572 and -305 mV , respectively meanwhile at pH of 5, the four dissolution peaks (a_1 , a_2 , a_3^* , and a_4^*) become at -921 , -759 , -476 and -399 mV respectively. These peaks correspond to the dissolution of the deposited metals from their different phases. The first one may be related to the dissolution of Zn from the pure zinc phase, which overlaps with the dissolution of Mn from its phases. The second two peaks are ascribed to the dissolution of Zn from its phases meanwhile the fourth one is attributed to the dissolution of Ni from its phases. It is apparent that when the pH is increased from 3 to 5, the first three anodic peaks shift towards the positive direction meanwhile the fourth one shifts towards the negative direction.

Generally, it is clear that the height of the peak (a_2) increases when the pH is increased from 2 to 5 accompanying with a shift towards the positive direction. The height of the peak (a_3) increases when the pH is increased from 1.5 to 5. The height of the peak (a_4) increases when the pH is increased from 1.5 to 2.5 followed by a decrease at pH of 3 then increase at pH of 5. It is obvious that the peaks (a_3 and a_4) have dissimilar behavior at pH of 5 where the peak (a_3) shifts towards the positive direction (becomes a_3^*) meanwhile the peak (a_4) shifts towards the negative direction (becomes a_4^*). This may be due to the weak acidity (pH= 5) of the electrolyte bath from which the alloy is obtained which perhaps lead to the formation of metal-oxidized species (oxides or hydroxides) in the interface and incorporation of them into the coating together with the metallic forms.

3.2 Galvanostatic measurements and ALSVs:

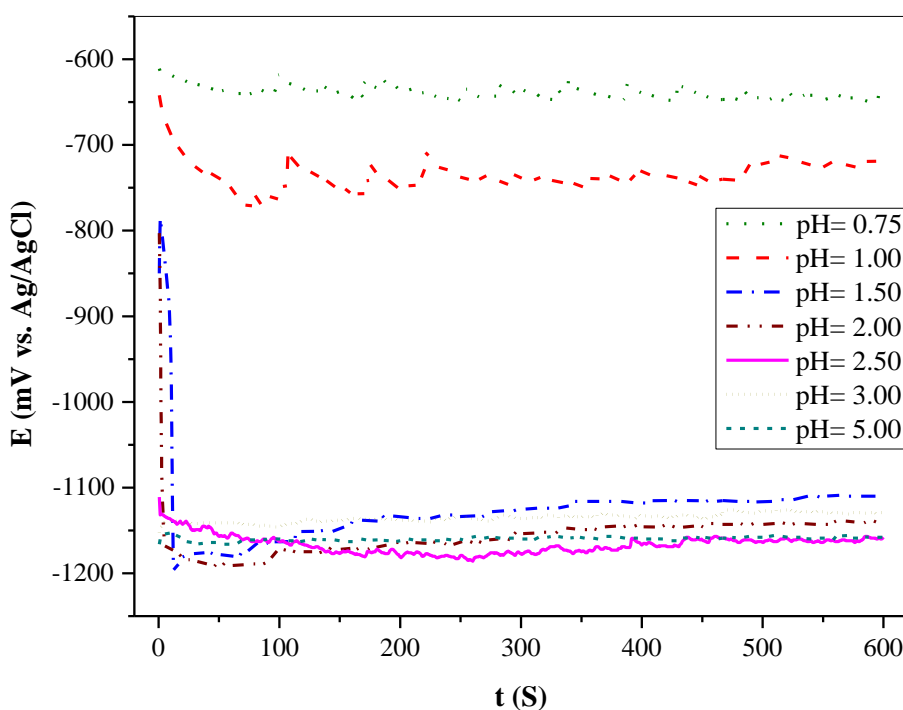


Figure 3. E - t curves for steel in a standard bath at 10 mA/cm^2 and $25.0 \text{ }^\circ\text{C}$ for 10 minutes at different pH values.

It is noteworthy that, the cathodic potential is the controlling factor during codeposition. The composition and quality of the alloys change as a result of changing the cathodic potential. [23] For monitoring the potential with time, galvanostatic curves are plotted in a static electrolyte under a constant current density (10 mA/cm^2). Figure (3) shows the potential-time dependence for the deposition of Zn-Ni-Mn alloys on steel rod at different pH values ranging from 0.75 to 5. At pH of 0.75 and 1, the deposition of the alloys occurs at low cathodic deposition potentials giving rise to obtaining Ni-enrich alloys since Ni needs low overpotential to create the initial nucleus indicating the

normal deposition at low pH values. The fluctuations in the galvanostatic curves at low pH values may be ascribed to the intense hydrogen evolution reaction accompanying nickel deposition. Muller et.al. had the same interpretation during the study the electrodeposition of zinc–nickel alloys from ammonium chloride baths at intermediate current densities and confirmed the obtained results. [1]

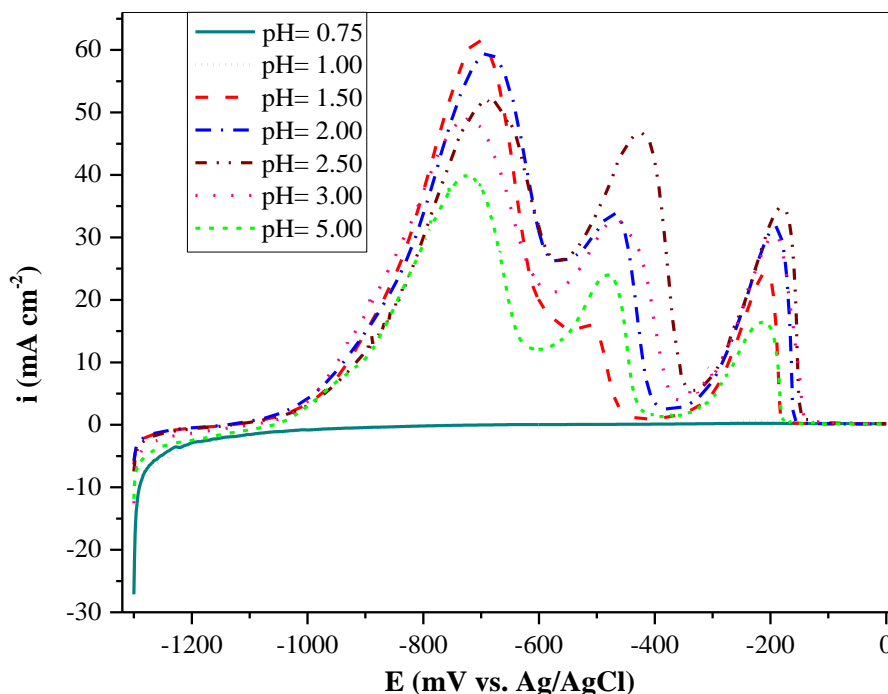


Figure 4. ALSVs for Zn-Ni-Mn alloys, obtained on steel rod at 10 mA/cm^2 and $25.0 \text{ }^\circ\text{C}$ for 10 minutes at different pH values from a standard bath, in $0.5 \text{ M Na}_2\text{SO}_4 + 0.05 \text{ M EDTA}$ at 5 mV/s and $25.0 \text{ }^\circ\text{C}$.

At pH of 1.5 and 2, the deposition potential shifts rapidly to more negative values during the first few seconds due to the nucleation process, then it slowly shifts to more positive values during the first minute till reaching a constant value during the remaining deposition time indicating that the alloy composition remains constant during the last deposition minutes. It is noticeable that the galvanostatic curves shift towards the cathodic direction as the pH value is increased from 0.75 to 2.5 then they shift positively at pH of 3 due to the decrease in the amount of deposited Zn and the increase in the amount of deposited Ni as indicated from Table (1) where the zinc content decreases from 89.8% to 83.5% and nickel content increases from 8.2% to 12.8% as the pH is increased from 2.5 to 5.

It is apparent that, the deposition potential at pH of 3 and 5 remains constant during all deposition time referring to that the alloy composition remains fixed during the growth process at these pH values. The sharp shift in the galvanostatic curves towards the negative direction when the pH is altered from 1 to 1.5 is due to the sharp increment in zinc content and a sharp decrease in nickel content as the pH is changed from 1 to 1.5. These results are in agreement with the values obtained in

Table (1) where the zinc content sharply increases from 29.7% to 94.1%, meanwhile the nickel content sharply decreases from 67.6% to 4.8% when the pH is increased from 1 to 1.5.

Figure (4) shows the anodic linear sweep voltammograms (ALSVs) obtained during the dissolution of Zn-Ni-Mn alloys electrodeposited at 10 mA/cm^2 at different pH values. At pH of 0.75, there are no any dissolution current peaks indicating that the only process which occurs during the deposition of the alloy at this pH value is the hydrogen evolution reaction which may be accompanied with the deposition of a very small amount of nickel that is not sufficient to bring the current density positive. At pH of 1, there is only one too small anodic peak at -227 mV , which is ascribed to the dissolution of Ni previously deposited on the steel substrate. The too small amount of the deposit obtained at very small pH values is correlated to the chemical dissolution of the deposit at high concentrations of sulfuric acid.

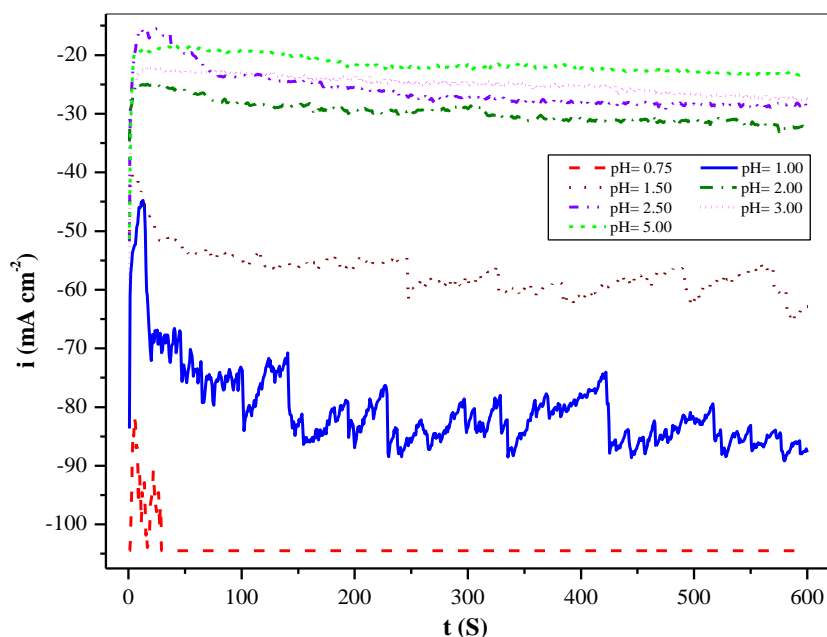


Figure 5. $i - t$ curves for steel in a standard bath at -1300 mV and $25.0 \text{ }^\circ\text{C}$ for 10 minutes at different pH values.

As the pH increases to 1.5, the dissolution of the alloys occurs under three voltammetric peaks. The first peak is related to the dissolution of Zn from pure zinc phase, the second one is attributed to the dissolution of Zn from $\gamma\text{-Ni}_5\text{Zn}_{21}$ and/or $\delta\text{-Ni}_3\text{Zn}_{22}$ phases and the third one is ascribed to the dissolution of Ni from its phases. It is noteworthy that there is no anodic peak related to Mn, which is not due to the non codeposition of manganese but due to the overlapping between the manganese dissolution peak from $\text{Mn}_{0.27}\text{Zn}_{0.73}$ or $\varepsilon\text{-ZnMn}$ phases and zinc dissolution peak from the pure zinc phase. This also may be ascribed to the low manganese content, as clear from Table (1), in the deposited alloys which is not sufficient to give a single clear dissolution peak. It is obvious that the height of the first anodic peak decreases as the pH is increased from 1.5 to 5 giving rise to the

decrease in pure Zn phase as the concentration of sulfuric acid is decreased. However, the height of the second and third anodic peaks increases as the pH is increased from 1.5 to 2.5 then it decreases as the pH has increased from 2.5 to 5.

According to the values of Zn, Ni and Mn amounts in the deposit given in Table (1) at pH of 2.5 and 5, the height of Zn dissolution peaks in the ALSVs are expected to be, at least, the same meanwhile the height of Ni dissolution peak at pH of 5 is expected to be higher than that at pH of 2.5. Moreover, it is expected that the alloy at pH of 5 will have more improved corrosion resistance properties than at pH of 2.5 due to the higher Ni content at pH of 5. As can be seen from the ALSVs at pH of 2.5 and 5, the reverse completely happens where the height of all anodic peaks at pH of 2.5 is higher than that at pH of 5 and all the anodic peaks at pH of 2.5 are at more noble potentials. This leads us to assume that some metal-oxidized species (oxides or hydroxides) are incorporated into the coating together with the metallic forms at pH of 5 due to the higher pH value and due to the increase in pH value at the electrode surface as a result of the hydrogen evolution reaction.

Taking into account that the coating at pH of 5 incorporates oxidized compounds, it is probably less compact and easier to oxidize so, the peaks at pH of 5 are at less noble potentials than at pH of 2.5 although the deposit at pH of 5 contains more Ni content. This agrees with what has been occurring to the third and fourth anodic peaks (a_3^* and a_4^*) in the cyclic voltammogram at pH of 5, Figure (1.b). It is very clear from Figure (4) that the alloy obtained at pH of 2.5 possesses the highest corrosion resistance properties because all the current dissolution peaks are at the most noble potentials. Moreover, the height of the second and third anodic current peaks are the highest indicating that the alloy has the highest content of γ -Ni₅Zn₂₁ and/or δ -Ni₃Zn₂₂ phases, which have more noble corrosion potentials than pure zinc phase, at this pH value.

3.3 Potentiostatic measurements and ALSVs

Figure (5) shows the current density-time dependence for the electrodeposition of Zn-Ni-Mn alloys on steel rod at -1300 mV for 600 seconds at different pH values ranging from 0.75 to 5. At pH of 0.75, there are fluctuations of large frequency and magnitude in the current density during the first 30 seconds, which may be due to the intense hydrogen evolution reaction over the steel substrate as a result of the very low pH value. After that, the current density remains constant indicating that the composition of the alloy remains unchanged during the remaining time. At the pH of 1, the current density increases rapidly to more positive values during the first 10 seconds because of the nucleation process. After that, the current density shifts to more negative values with occurring fluctuations of high frequency and magnitude referring that the composition of the alloy is changing during the growth time resulting in obtaining non homogeneous coatings at this low pH value. W. Lu et. Al. concluded that the films of FeCo prepared at low pH values shows a very poor quality with rough surface and the surfaces of the films electrodeposited at high pH value are generally quite smooth, uniform and compact. [16]

As the pH is increased from 1 to 5, the potentiostatic curves shift towards the positive direction which may be due to the increment in the content of the Zn and Mn. Furthermore, the fluctuations in

the potentiostatic curves decrease due to the decrease in the reduction of hydrogen ions. It is clear from the figure that there is a large shift in the current density towards the positive direction as the pH is increased from 0.75 to 2 then a small shift as the pH is increased from 2 to 5. Also, it is noticeable that the cathodic current density remains constant after the nucleation process at the pH values from 2 to 5 giving rise to the deposit composition remains constant during its growth at these pH values.

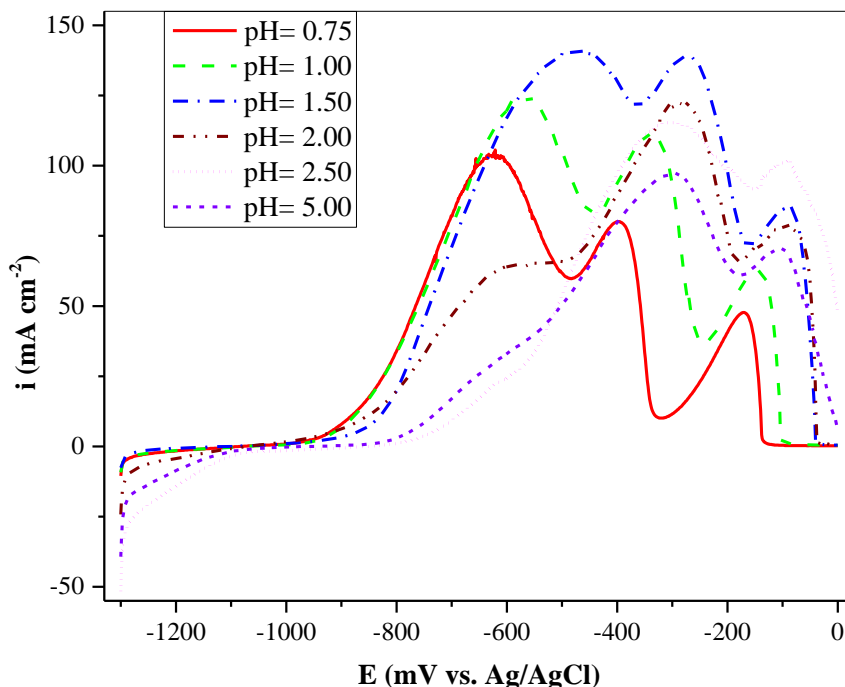


Figure 6. ALSVs for Zn-Ni-Mn alloys, obtained on steel rod at -1300 mV and 25.0 °C for 10 minutes at different pH values from a standard bath, in 0.5 M Na₂SO₄ + 0.05 M EDTA at 5 mV/s and 25.0 °C.

Figure (6) shows the ALSVs obtained during the dissolution of Zn-Ni-Mn alloys electrodeposited at -1300 mV for 10 minutes at different pH values ranging from 0.75 to 5. At a pH of 0.75, there are three anodic dissolution peaks corresponding to the dissolution of the alloy metals from their phases. As the pH is increased from 0.75 to 1.5, the height of the anodic peaks increases indicating the increment of the alloy components. Moreover, the peaks shift towards the positive direction, giving rise to the improvement of the corrosion resistance properties. At pH value of 2, there is a sharp decrease in the height of the first dissolution peak giving rise to the sharp decrease in the content of pure Zn phase. Also, there is a small decrease in the height of the second and third dissolution peaks giving rise to the small decrease in the content of γ -Ni₅Zn₂₁ and/or δ -Ni₃Zn₂₂ phases. At pH values of 2.5 and 5, the ALSVs begins to take abnormal shapes where the first anodic peak begins to overlap with the second anodic peak. Moreover, the current density does not reach zero value at the end of the oxidation process indicating that the deposit is not completely removed from the electrode surface.

From Figure (4) and Figure (6), it is clear that there is a large difference between the behavior of the coatings deposited under galvanostatic conditions and those deposited under potentiostatic conditions, particularly at low pH values (pH of 0.75 and 1) where the content of the coating components obtained galvanostatically is too low compared to that obtained potentiostatically as obvious from the height of the anodic peaks for the coatings obtained at pH values of 0.75 and 1. This may refer to that the low acidity of the electrolyte does not affect the deposits obtained potentiostatically but affects (dissolves) the deposits obtained galvanostatically. Furthermore, at the same pH value, the peaks of the coating obtained potentiostatically are at more noble potentials than those obtained galvanostatically giving rise to the better corrosion resistance properties of the coatings obtained potentiostatically as same pH value.

3.4 Potentiodynamic polarization measurements

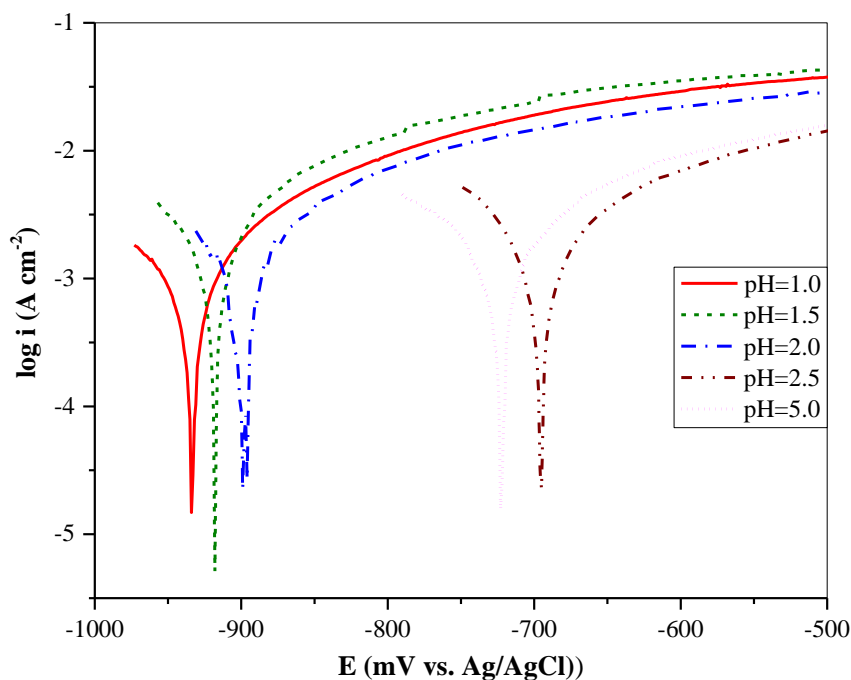


Figure 7. $\log i - E$ curves for Zn-Ni-Mn alloys, obtained on steel rod at -1300 mV and 25.0 °C for 10 minutes at different pH values from a standard bath, in 0.05 M HCl at 5 mV/s and 25.0 °C.

Figure (7) shows the potentiodynamic polarization curves for Zn-Ni-Mn alloys obtained potentiostatically at -1300 mV for 10 minutes over a steel rod at different pH values. As can be seen from the figure, the alloys have more negative corrosion potentials at pH values of 1, 1.5 and 2 indicating the low corrosion resistance properties. At pH values of 2.5 and 5, the alloys possess more noble corrosion potentials giving rise to the improvement of the corrosion resistance properties of the alloys obtained at these pH values. It is noticeable that there is a sharp shift in the measured corrosion

potential towards the positive direction when the pH is altered from 2 to 2.5 referring to the sharp change in the composition of the obtained alloys as a result of this alteration. It is clear from the same figure that the best pH value of obtaining a coating possessing the best corrosion resistance properties is 2.5. Ni slightly decreases, as mentioned by X. Su and C. Qiang during the study of electrodeposition of Ni-Fe, [14] as the pH values increase and confirmed the preset work (pH = 1-1.5). But, in this work Ni started again to increase as the pH values increase from 2.5 to 5.

3.5 Surface morphology

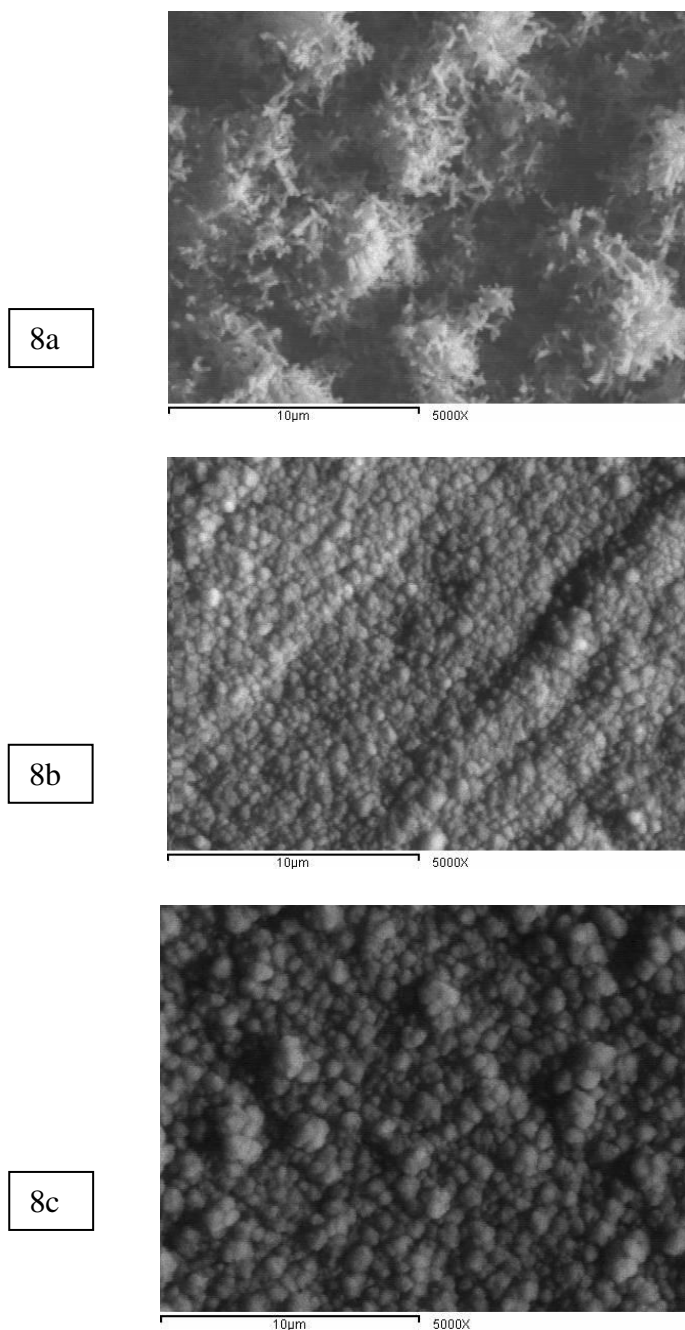


Figure 8 a, b and c. SEM micrograph for Zn-Ni-Mn alloy electroplated on steel substrate of area 2 cm^2 at 10 mA/cm^2 and $25.0 \text{ }^\circ\text{C}$ for 10 minutes at pH values of (a) 1.5, (b) 2.5 and (c) 5.0 from a standard bath.

Figures (8.a, b and c) show the scanning electron microscope (SEM) micrographs for Zn-Ni-Mn alloys obtained on steel substrate at 10 mA/cm^2 for 10 minutes at pH values of 1.5, 2.5 and 5.0. At pH of 1.5, the surface morphology of the deposit is rough, non-homogeneous, non-crystalline and non-uniform resulting in the deposit possesses low compactness, low hardness and low adherence. This may be due to the inclusion of hydrogen atoms into the deposit during its growth, causing embrittlement for it or may be due to the effect of the high concentration of sulfuric acid on the coating. In addition, the morphology of the deposit has changed to a uniform fine grain size at pH 2.5. At a pH of 5.0, the coating becomes crystalline, homogeneous and uniform. Therefore, the coating will be compact, adherent and hard when it grows in slightly acidic solutions. The same results obtained by X. Su and C. Qiang [14] and they concluded that the Ni-Fe films grown in high pH values have larger grains compared to those prepared at low pH values.

3.6 Electrochemical measurements and deposit composition

Table 1. Values of Zn, Ni and Mn amounts, total mass, content% of Zn, Ni and Mn, current efficiencies of Zn-Ni-Mn deposits, thickness and electrochemical corrosion measurements of the deposits obtained galvanostatically at 10 mA/cm^2 and $25.0 \text{ }^\circ\text{C}$ for 10 minutes at different pH values on 2 cm^2 area of steel substrate from a standard bath.

Parameter	pH			
	1	1.5	2.5	5
Zn amount in the deposit $\times 10^{-4} / \text{g}$	0.11	25.50	31.70	31.30
Ni amount in the deposit $\times 10^{-4} / \text{g}$	0.25	1.30	2.90	4.80
Mn amount in the deposit $\times 10^{-4} / \text{g}$	0.01	0.30	0.70	1.40
Total mass of the deposit $\times 10^{-4} / \text{g}$	0.37	27.10	35.30	37.50
Zn content / %	29.70	94.10	89.80	83.50
Ni content / %	67.60	4.80	8.20	12.80
Mn content / %	2.70	1.10	2.00	3.70
Zn-Ni-Mn alloy current efficiency ($e_{\text{Zn-Ni-Mn}}$) / %	0.98	67.10	87.90	94.20
Thickness of the deposit / μm	0.023	1.90	2.47	2.64
Corrosion potential ($E_{\text{corr.}}$) / mV	-934	-918	-695	-722
Corrosion current density ($i_{\text{corr.}}$) / $\mu\text{A cm}^{-2}$	31.30	28.20	13.60	17.40
Polarization resistance (R_p) / $\text{k}\Omega$	6.67	7.29	12.64	10.95

Table (1) explains the dependence of Zn-Ni-Mn alloy composition of the pH value at which the alloy is obtained. At pH value of 1, the alloy contains 29.7% of Zn, 67.6% of Ni and 2.7% of Mn

giving rise to normal codeposition. This indicates that Ni can resist the corrosive media (sulfuric acid) more than Zn and Mn due to its low chemical reactivity with respect to the reactivity of Zn and Mn. In other words, the dissolution action of H_2SO_4 acid on the deposited Ni is less than that on Zn and Mn. As the pH value increases to 1.5, the Zn content increases sharply meanwhile the Ni content decreases sharply referring to the beginning of the anomalous codeposition. As the pH is increased from 1.5 to 5, the Zn content decreases from 94.1% to 83.5%, while the Ni and Mn contents increase from 4.8% to 12.8% and from 2.7% to 3.7% respectively. It is clear that we can control the type of deposition, i.e. normal or anomalous, by changing the pH value of the electrolyte.

At pH values of 1, the current efficiency is too low, indicating that the main reaction which occurs on the cathode surface at this pH value is the hydrogen evolution reaction. The too low efficiency is also due to the chemical dissolution of the deposit by the action of the highly corrosive medium (H_2SO_4 acid). As the pH is increased from 1.5 to 5, the current efficiency of all alloy components increases (except for Zn at pH 5 where it slightly decreases) resulting in the increment of the alloy efficiency of 67.1% at pH of 1.5 to 94.2% at pH of 5. It is clear that there is a sharp increment in the alloy current efficiency when the pH is altered from 1 to 1.5 due to the sharp increment in the Zn current efficiency.

The obtained results (Table 1) clarify that the thickness of the deposited alloy increases as the pH value is increased because of the increment in the content of alloy components. The abrupt increment in the coating thickness when the pH value is increased from 1 to 1.5 is due to the decrease in the corrosive medium action on the obtained coating. It is clear that the thickness of the obtained coating does not significantly increase after the pH value of 2.5.

The electrochemical corrosion measurements (Table 1) reveal that at pH 2.5 the deposit has the highest polarization resistance and the lowest corrosion current and the more positive corrosion potential.

4. CONCLUSION

The electrodeposition of Zn–Ni–Mn exhibited the phenomenon of anomalous type codeposition at the studied pH values from 1.5 to 5. On the other hand, normal codeposition was attained at lower pH values (<1.5). The increase in pH value from 1.5 to 5, leads to a little decrease in the anomalous behavior. At pH 1.5 the surface morphology of the deposit is rough, non-homogeneous, non-crystalline and non-uniform resulting in the deposit possesses low compactness, low hardness and low adherence. In addition, the morphology of the deposit has changed from a uniform fine grain size at pH 2.5 into a higher grain size at pH 5. Also, the current efficiency of the alloy decreases with a higher H_2SO_4 concentration because of the increase of the hydrogen evolution. In conclusion, the optimal pH value (2.5) is required to attain better surface coverage with fine grained structure, moderate current efficiency, and the highest corrosion resistance.

References

1. C. Muller, M. Sarret, and T. Andreu, *Electrochim. Acta*, 48(17) (2003) 2397
2. M.E. Bahrololoom, D.R. Gabe, and G.D. Wilcox, *J. Electrochem. Soc.*, 150(3) (2003) C144
3. J.B. Bajat, V.B. Mišković-Stanković, M.D. Maksimović, and D.M. Dražić, *Electrochim. Acta*, 47(25) (2002) 4101
4. H.A. Sorkhabi, A. Hagrah, N.P. Ahmadi, and J. Manzoori, *Surf. Coat. Technol.*, 140(3) (2001) 278
5. R. Ramanauskas, L. Gudavičiūtė, A. Kaliničenko, and R. Juškėnas, *J. Solid State Electrochem.*, 9(12) (2005) 900
6. J.F. Huang and I.W. Sun, *J. Electrochem. Soc.*, 151 (2004) 8
7. H. Dahms and I. M. Croll, *J. Electrochem. Soc.*, 112 (8) (1965) 771
8. H. Fukushima, T. Akiyama, M. Yano, T. Ishikawa and R. Kammel, *J. ISIJ Int.*, 33 (9) (1993) 1009
9. T. Osaka, M. Takai, K. Hayashi, K. Ohashi, M. Saito and K. Yamada, *Nature*, 392 (6678) (1998) 796
10. C. Müller, M. Sarret, and M. Benballa, *Electrochim. Acta*, 46(18) (2001) 2811
11. C. Savall, C. Rebere, D. Sylla, M. Gadouleau, Ph. Refait, and J. Creus, *Mater. Sci. Eng. A*, 430(1-2) (2006) 165
12. M. Bučko, J. Rogan, S.I. Stevanović, A. Perić-Grujić, and J.B. Bajat, *Corros. Sci.*, 53(9) (2011) 2861
13. A. Bai and C. Hu, *Electrochimica Acta*, 47 (2002) 3447
14. X. Su and C. Qiang, *Bull. Mater. Sci.*, 35(2) (2012) 183
15. T. Mahalingam, K. Sundaram, S. Velumani, M. Raja, S. Thanikaikarasan, Y. Kim and R. Asomoza, *Advanced Materials Research*, 68 (2009) 52
16. W. Lu, C. Ou, P. Huang, P. Yan and B. Yan, *Int. J. Electrochem. Sci.*, 8 (2013) 8218
17. M.M. Abou-Krishna, *J Appl Surf Sci*, 252 (2005)1035
18. T. Ohtsuka, E. Kuwamura, A. Komori and T. Uchida, *ISIJ Int.*, 35 (1995) 892
19. M.M. Abou-Krishna, H.M. Rageh and E.A. Matter, *Surf. Coat. Technol.*, 202 (2008) 3739
20. M.H. Seo, D.J. Kim and J.S Kim, *Thin Solid Films*, 489 (2005) 122
21. Y. Lin and J.R. Selman, *J. Electrochem. Soc.* 140 (1993) 1299
22. M.M. Abou-Krishna, F.H. Assaf and A.A. Toghian, *J Solid State Electrochem*, 11 (2007) 244
23. A.G. Dolati, M. Ghorbani and A. Afshar, *Surf. Coat. Technol.* 166 (2003) 105

© 2015 The Authors. Published by ESG (www.electrochemsci.org). This article is an open access article distributed under the terms and conditions of the Creative Commons Attribution license (<http://creativecommons.org/licenses/by/4.0/>).